

IMPACT MODELLING OF WIND FARMS ON MARINE NAVIGATIONAL RADAR

L. S. Rashid, A.K. Brown

MACS Engineering Research Group
School of Electrical & Electronic Engineering
University of Manchester, UK

Keywords: Marine Radar, Wind Farms, Siting.

Abstract

The impact of wind turbines on radar systems is of increasing concern. This paper addresses the problem of the offshore wind farm and presents a methodology used to model the interference of wind turbines with pulsed marine navigational radar. It will show the ability to model some of the main issues such as; target spreading, sidelobe detection and the appearance of ghost targets. A comparison between the results from the model and measured data taken near the North Hoyle wind farm in North Wales, UK is provided.

1 Introduction

Offshore wind farm technology is expected to make a significant contribution to meeting the UK Government target of 10 per cent of the country's electricity needs through renewable sources by 2010 [8].

Offshore wind farms cover large areas of open water and hence present potential hazards to navigation. A number of potential sites are considered to be close to or encroach into waters with a high density of shipping movements or waters used by fishing vessels and recreational craft. Their positions are necessarily those which are exposed to weather conditions which could affect the navigation of vessels, particularly small craft [4]. Investigation into the interference by wind farms with ships' radar has confirmed that there may be an impact on radar producing spurious returns on displays caused by multiple reflections, as well as beam spreading and side-lobe detection due to the very high radar cross section of the wind turbine [2].

Unlike air traffic control radars, marine navigational radars are low complexity/cost. The practicality of introducing advanced signal processing into these radars to reduce wind farm impact is considered unlikely [12,13]. Therefore the requirement exists to determine likely effects of a specific wind farm on marine radar prior to construction.

The wind farm impact on marine radars has not been widely reported. Some past publications have touched on the subject [4,8,14] but there has been no accurate model in place to readily examine the effects of different farm geometries, tower shapes and turbine sizes.

This paper discusses the radar modelling of offshore wind farms including the methods used to model individual turbine mono and bi-static RCS, the propagation medium and the multiple reflections of radar signals within the wind farm. An initial qualitative comparison between the results of the model and measured data is provided

2 The Wind Turbine Model

Wind turbines are large structures that are typically made of GRP and/or carbon fibre composite components mounted on steel towers. Full physical optics modelling [1,5,9] of a typical turbine shows that the RCS can be in the order of 60 dBms (10^6 m^2) at 9.4 GHz which is of the same order as a large oil tanker broadside on.

Pinto [9] shows results of a full physical optics modelling of a wind turbine. This shows the variation in RCS with respect to the rotation angle of the blades and the yaw angle as defined in Figure 1.

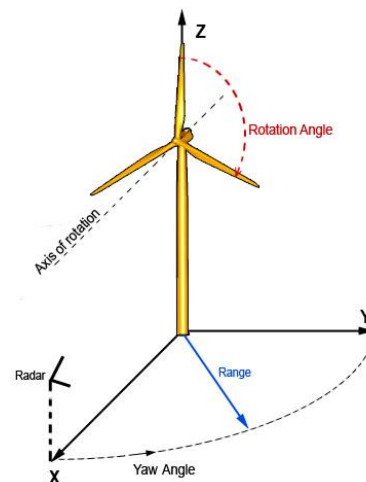


Figure 1: RCS modelling coordinate system

It was found that the tower constitutes by far the largest source of scatter (approx. 80%) followed by the blades (5% each). The nacelle was only considered to be a significant source of scatter for 90° yaw case (i.e. broadside on). The nosecone was found to be largely insignificant at all angles [8].

The problem of utilising the physical optics model for a flexible wind farm calculation is largely one of scale. Current generation of wind farms use turbines with blade lengths of

approximately 30 to 40m (60 to 80-m diameter) on a tower of height 70m. This is likely to grow with 160m diameter a future possibility. As marine navigational radar operate up to X-band, the electromagnetic size of the RCS calculation is already large (many thousands of wavelengths) with the blades of complex shape. While RCS prediction of this size is possible clearly it is non trivial. An additional problem is in a wind farm adjacent turbines are in the near field of their neighbours and may be in the near field of the ship's radar antenna. This significantly increases computational effort.

Accordingly a simplified, approximate model has been developed to compute the monostatic and bistatic RCS of the tower as the dominant component and combined with the PO model of the blade to provide a rapid calculation tool capable of positioning the blades at any rotation/yaw angle.

The turbine was split into sections. The section size ensures that a far field approximation from each section can be used. The RCS values for sections including the nacelle, the blades and the nosecone across all yaw and rotation angles were taken from a full PO model, so that the shape of the blade is accurately taken into account. Each section is then assumed as a point scatterer positioned at the centre the relevant section.

2.2 Tower RCS Model

The tower is modelled as a set of cylindrical sections as shown in Figure 2 below. By segmenting the tower into small cylindrical sections, the nearfield RCS can be calculated providing the effective scattering centre for each section is known.

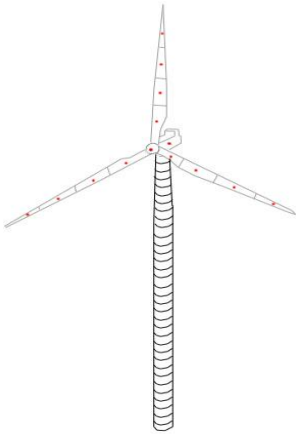


Figure 2: Segmented turbine model

We note both mono- and bi-static RCS prediction is required: The monostatic RCS of the tower is used to investigate issues such as the target spreading and side-lobe detection, while the bistatic RCS is required to predict the appearance of ghost targets due to multiple reflection issues.

The RCS of each section was obtained using standard simplified physical optics farfield RCS approximations of a cylinder [6] given in Equation (1).

$$\sigma_{\text{mono}} = krh^2[\cos(\varphi_n) \text{sinc}(kh/2\sin \varphi_n)]^2 \quad (1)$$

The phase reference point of each section is assumed to be at the surface of the cylindrical section since the section diameters are very large compared to the wavelength of the radar signal. With information about the radar height and the range, the distance to each segment d is calculated which is used to account for the phase contribution of individual segments.

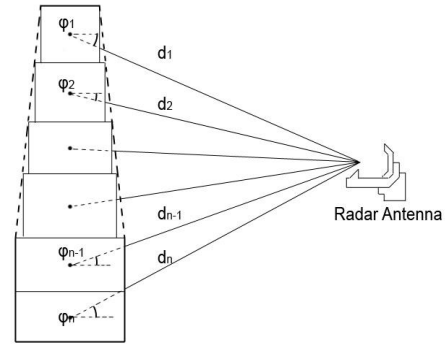


Figure 3: Segmented tower geometry.

Figure 3 shows a simplified segmented tower. Using the approximation discussed above, the complex field V_n value at any required for each segment is simply

$$V_n = [\sigma_n/(d_n/R)^2]^{1/2} \quad (2)$$

A complex summation over all segments leads to the required total RCS at a defined point.

For the bi-static case the RCS of each section is taken as (see Figure (4)) [10]

$$\sigma_{\text{bi}} = krh^2[\cos^2\varphi_2\cos(\theta/2)/\cos\varphi_1] \text{sinc}^2[kh/2(\sin\varphi_1+\sin\varphi_2)] \quad (3)$$

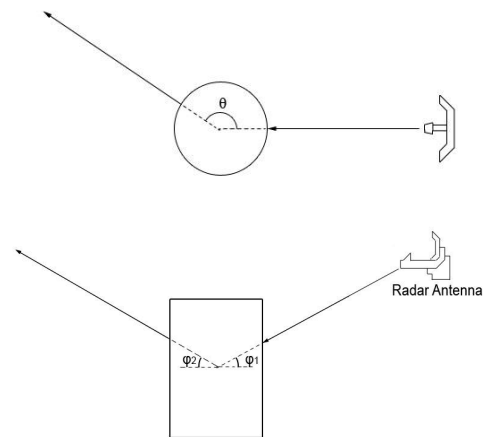


Figure 4: Bistatic RCS Layout

Similar to the monostatic RCS, by using Equation (3) to obtain the amplitude of the RCS and the distance d to account for the phase contribution, Equation (2) is then used to find the field V_n value at that point for each segment. This is then added to the rest of the contributions from the other segments to calculate the total bistatic RCS of the tower to a given direction.

2.2 Multiple Bounce Model

When ships are near a wind farm spurious targets appear on the radar display. This phenomenon occurs due to the multiple reflections of radar signals within the farm. A ray tracing model has been implemented which calculates successful ray directions from the ship radar to each tower and the direction from any one tower to any other. The monostatic and bistatic RCS of the tower in the required directions is then obtained from the above model and the field reflected or diffracted to the next tower calculated.

The model uses a recursive technique whereby the reflected signal off the tower is traced through as many bounces needed until it reaches a defined threshold value below which it is considered insignificant. The model also allows for potential multiple bounces both from any tower to any other tower and from a nearby ship to the towers.

Finally the ray tracing model allows for multiple wanted targets in addition to the wind farm to be introduced.

Sea clutter effects are included based on the GIT empirical models [3,7,11], in addition a single point sea surface multipath reflection is included.

3 Results

The results of the model can be divided into two sections: Turbine RCS model results and Radar impact model.

In order to validate the turbine RCS model, the results were compared to the full physical optics model provided by BAESystems. Figure (5) below shows the variation of the RCS around the turbine while maintaining the rotation angle at 0°.

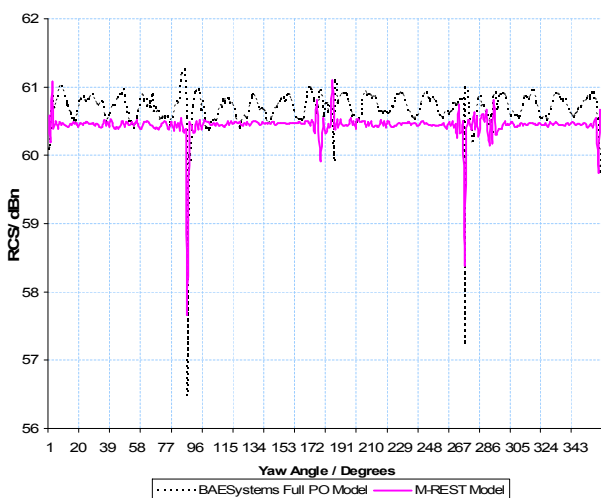


Figure 5: RCS variation around the turbine (Rotation = 0°)

The model shows a good correlation with the full PO model. At 180° the model peaks slightly higher than the PO model due to the shadowing effect from the tower and the nacelle, which is not included.

Figure (6) below shows the variation of the RCS with the rotation angle while keeping the yaw angle at 0°. The correlation between the PO model and the developed model is good. The variations in the plots are due to the fine meshing of the blades, nacelle and the nosecone in the PO model which gives accurate phase contributions, while the developed model assumes point scatterers with phase reference positioned at the centre of each section as shown in figure (2).

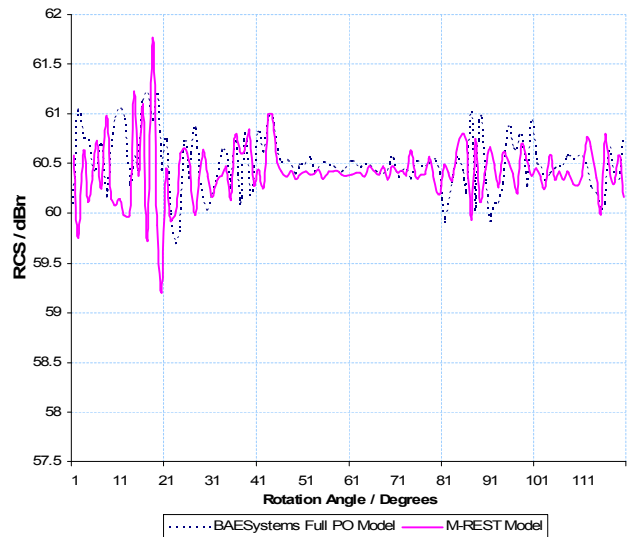


Figure 6: RCS variation with rotation (Yaw = 0°)

To illustrate the impact of wind farms on marine radar, the output of the model is in the form of a synthetic scan-converted display showing the radar returns in a colour coded scale.

The impact model has been compared to some available radar display images taken when visiting an offshore wind farm in North Wales.

The navigational radar employs a simple video processing algorithm. It was also set to have an “automatic gain” setting to adjust the threshold setting and the gain of the receiver. This was modelled by manually adjusting the receiver threshold.

Figure (7a) shows the actual radar display detection of wind turbines through the side lobes when the vessel was near the wind farm.

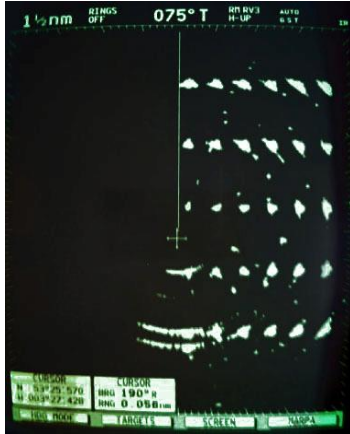


Figure 7a: measured data showing sidelobe detection and target spreading

When this scenario was modelled using the developed model, the locations of the wind turbines was set as closely as possible to that in the measurement. The output of the model shows the power received as shown in Figure 7 (b). There is a significant detection through the side lobes. The locations of these returns are very similar to that in the measured data.

Differences in the detailed level of the side lobe detections may be caused by using an estimated azimuth antenna pattern rather than a measured pattern. The model also does not use any video processing algorithms or automatic gain and thresholding settings.

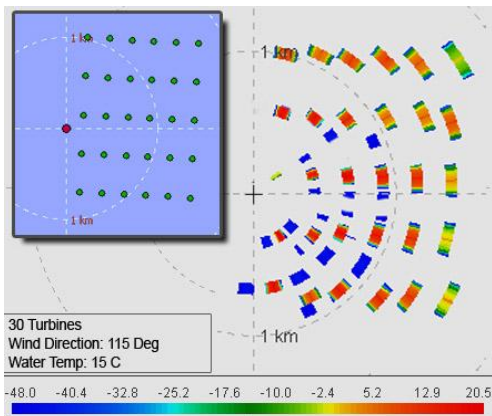


Figure 7b: model results showing sidelobe detection and target spreading

Multiple reflections of the radar signal within the wind farm can cause the appearance of ghost targets on the radar screen. Figure 8 (a) is a picture of the actual radar display showing the effect. The results of modelling that scenario are shown in Figure 8 (b) where a good quantitative correlation between the model and the measurement is clear.

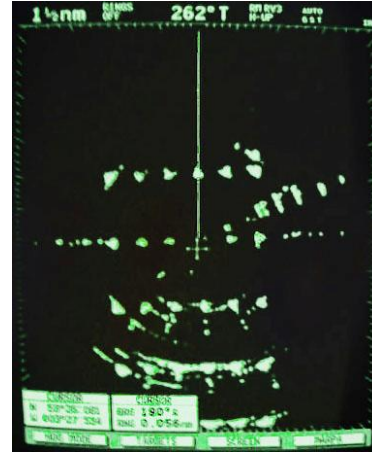


Figure 8a: measured data showing the appearance of ghost targets.

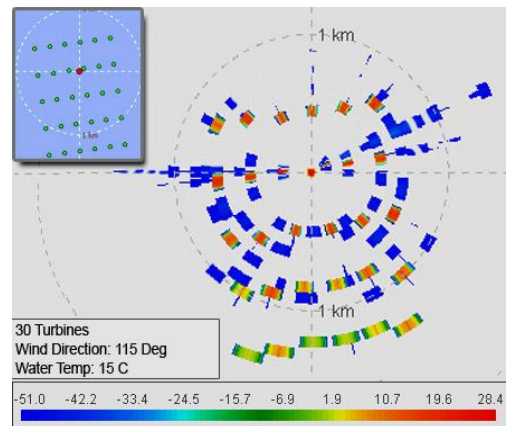


Figure 8b: model results showing the appearance of ghost targets.

4 Conclusion

Offshore wind farm locations, which cover large areas of open waters, may present navigational hazards to marine traffic. Some of these concerns arise from the interference of wind turbines with the shipborne and onshore VTS stations radars.

The radar model developed at the University of Manchester is designed to give a flexible, rapid and reasonably accurate calculation for application to a wide variety of wind farms. Initial comparison of results with measurements, demonstrates the ability to simulate the interference of wind farms with navigational radars. Further work is required to further validate predictions; however, it has a good qualitative correlation with pictures of a shipborne radar screen taken at the North Hoyle wind farm.

Acknowledgements

This work has been partially funded by a DTI innovation award (No. TP/2/RT/6/1/10117 APPS2B) which is a collaboration between BAESystems Ltd, Vestas a/s, University of Sheffield and University of Manchester. The help of our partners is gratefully acknowledged.

References

- [1] S Appleton, "Stealthy Wind Turbines - addressing the radar issue", *BWEA28*, (2006).
- [2] R Baker. "BWEA Marine Radar Investigation", *BWEA28*, (2006).
- [3] D K Barton, Radar System Analysis and Modeling. Boston: Artech House, 2005
- [4] C Brown, M. Howard, "Results of the electromagnetic investigations and assessments of marine radar, communications and position fixing systems undertaken at the North Hoyle wind farm by QinetiQ and the Maritime and Coastguard Agency", *MCA Report MNA 53/10/366*, Nov 2004.
- [5] H S Dabis, "Wind Turbine Electromagnetic Scatter Modelling using Physical Optics Techniques", *Renewable Energy*, **16** pp. 882-887, (1999).
- [6] E F Knott, J F Shaeffer and M T Tuley, Radar Cross Section, 2nd edition. Boston: Artech House, 1993
- [7] M L Meeks, Radar Propagation at Low Altitudes. Boston: Artech House, 1982
- [8] J Pinto, A. K. Brown, L. Rashid, Z. Moore, "Requirements Capture Summary Report", Stealth Technology for Wind Turbines, TP/2/RT/6/I/10117 APPS2B, April 2006
- [9] J Pinto. "Stealth Technology for Wind Turbines - Addressing the Aviation and Marine Radar Issues", *BWEA28*, (2006).
- [10] G T Ruck, D E Barrick, Radar Cross Section Handbook, Vol 1. New York: Plenum Press, 1970
- [11] M I Skolnik, Introduction to Radar Systems, 2nd edition. New York: McGraw-Hill Book Company, 1980
- [12] C Trundle, "Primary Radar v Wind Farms: Safety Case Mitigation", *BWEA28*, (2006).
- [13] D M Webster, "The Effects Of Wind Turbine Farms On ATC Radar", AWC/WAD/72/665/TRIALS, MAY 05.
- [14] D A Zolnick, "Calculating the Radar Cross Section from multiple Bounce Interaction", *Naval Research Labs*, USA (1993).